2018

Soft Microreactors for the Deposition of Conductive Metallic Traces on Planar, Embossed, and Curved Surfaces

Abhiteja Konda

Advaith Rau

Michael A. Stoller

Jay M. Taylor

Abdul Salam
Purdue University, salama@purdue.edu

See next page for additional authors

Authors
Abhiteja Konda, Advaith Rau, Michael A. Stoller, Jay M. Taylor, Abdul Salam, Gabriel A. Pribil, Christos Argyropoulos, and Stephen A. Morin

DOI: 10.1002/adfm.201803020

Article type: Full Paper

Soft Micro-reactors for the Deposition of Conductive Metallic Traces on Three-dimensional Objects

Abhiteja Konda,[a] Advaith Rau,[a] Michael A. Stoller,[a] Jay M. Taylor,[a] Abdul Salam,[b] Gabriel A. Pribil,[a] Christos Argyropoulos,[cd] and Stephen A. Morin[ad]*

[a] Abhiteja Konda, Advaith Rau, Michael A. Stoller, Jay M. Taylor, Gabriel A. Pribil, Prof. Stephen A. Morin
Department of Chemistry, University of Nebraska – Lincoln, Lincoln, NE 68588, USA.
E-mail: smorin2@unl.edu

[b]Prof. Abdul Salam
Department of Computer and Information Technology, Purdue University, West Lafayette, IN 47907, USA.

[c] Prof. Christos Argyropoulos
Department of Electrical and Computer Engineering, University of Nebraska – Lincoln, Lincoln, NE, 68588, USA

[d]Prof. Christos Argyropoulos, Prof. Stephen A. Morin
Nebraska Center for Materials and Nanoscience, University of Nebraska – Lincoln, Lincoln, NE 68588, USA.

Keywords: microfluidics, electroless deposition, functional coatings, patterned metallization, 3D circuits

Advanced manufacturing strategies have enabled the large-scale, economical, and efficient production of electronic components that are an integral part of various consumer products ranging from simple toys to intricate computing systems; however, the circuitry for these components is (by and large) produced via top-down lithography and is thus limited to planar surfaces. The present work demonstrates the use of reconfigurable soft micro-reactors for the

patterned deposition of conductive copper traces on flat and embossed 2D substrates as well as 3D substrates made from different commodity plastics. Using localized, flow-assisted, low-temperature, electroless deposition, copper traces were deposited, which, when combined with various off-the-shelf components, enabled the fabrication of simple electronic circuits and antennas. The application of this solution-phase method to the patterned deposition of functional inorganic materials selectively on different 2D/3D polymeric substrates will provide simple, inexpensive processing opportunities for the fabrication of electronic devices with non-traditional form factors when compared to relatively complicated manufacturing methods such as laser-directed structuring. Further, this approach to the patterned metallization of different commodity plastics offers unique design opportunities applicable to the fabrication of 3D traces and interconnect devices, and other free-form electronics with less structural "bloat" and weight (by directly coating support elements with circuitry and thus eliminating the need for dedicated circuit boards).

1. Introduction

Despite the advanced capabilities of top-down lithography in processing a diversity of materials with a range of functionalities (e.g., electronic, magnetic, etc.), it remains a challenge to adapt these processes to the precise placement/deposition of materials on non-planar and three-dimensional (3D) surfaces. In the present work, we wish to design a process that simplifies the rational deposition of conductive traces on non-planar and 3D surfaces, is compatible with commercial materials (e.g., structural commodity plastics), and that is broadly useful for many applications (e.g., 3D circuits, free-form electronics, etc.).

Specifically, we used soft, bi-layered stretchable microfluidic reactors, which take advantage of the compressibility of elastomeric materials to create reversible seals,[1] to deposit conductive metallic traces, directly, onto flat polymer surfaces with textured finishes, relief patterns, as well as those with 3D features/geometries via localized, flow-assisted, solution-phase electroless deposition. This approach has two unique characteristics: (i) desired patterns of conductive traces can be generated through the rational design of the channel network within the soft reactors, and (ii) necessary additions to the patterned traces that are needed to complete a circuit can be achieved by reorienting the soft micro-reactor (or reactors of different designs) for successive depositions (or etching steps). Further, we demonstrated that the deposited traces, in combination with various off-the-shelf components, enabled the fabrication of planar/non-planar circuits of different functionalities (e.g., LED displays, simple detectors, and antennas). The ability to selectively deposit functional inorganic materials (the focus in this work was conductive copper traces, but other materials are potentially accessible using different chemistry) using flow-based, low-temperature, aqueous-phase synthesis can provide alternative manufacturing techniques that offer simple, inexpensive processing opportunities, especially for the fabrication of devices with non-planar form factors. For example, this approach can be used to fabricate 3D electronic circuits and antennas for communication devices, biomedical instruments, and automotive components with greater flexibility in their space-filling geometries.

Metallization of plastics imbibes the useful electric, magnetic, and inductive properties of metals to these materials. Compared to electroplating,[2] which may result in the build-up of material at the edges and corners of the target substrate, and requires power supplies and conductive substrates, electroless plating has several advantages: it (i) is a simple one-pot, solution-based approach that uses a redox reaction to deposit metal directly, (ii) is cost effective, as it does not involve power supplies and other instrumentation, (iii) is applicable to the generation of uniform coatings on complicated shapes, and (iv) is able to coat non-conductive substrates, such as plastics and polymers.[3] In addition to its ability of metallizing non-conductive surfaces (e.g., polymers), electroless deposition has key practical advantages over other popular metallization techniques, such as chemical vapor deposition,[4] thermal spray methods,[5] and physical vapor deposition,[6] including: the ability to (i) deposit inorganic material selectively on the substrates without the need for lithography, and (ii) operate using simple, low-cost processing equipment. These characteristics make electroless deposition applicable to a diversity of substrates including metals, numerous plastics (e.g., polycarbonate, acrylonitrile-butadiene-styrene),[3,7] glass,[8] and elastomeric materials.[9] The metallization of polymers or plastics, as a mature subset of electroless deposition in general, is critical to the fabrication of PCBs that are ubiquitous in electronics, and more generally to the manufacture of, for example, decorative or protective coatings, packaging paper, etc.[10]

Electroless copper deposition (ECD, which is the focus of this work) generally involves three essential steps: surface pre-treatment, activation, and deposition (Fig. S1, see S.I. text).[11] Several pre-treatment methods have been reported to improve the adhesion of the metal particles to the polymeric substrate, including the use of plasmas, lasers,[12] and chemical etching. Activation of the surfaces, which simultaneously aids adhesion and promotes film formation, has been achieved using colloidal seed layers that provide favorable sites for copper nucleation and growth in subsequent deposition step, where Pd-Sn seeds are established activator particles that have proven to be highly effective for enhancing copper deposition.[13]

ECD can be applied to the formation of 3D metal traces and interconnect devices that enable non-traditional forms of electronic devices. This 3D ECD is typically achieved following substrate activation that is based on 3D, patterned laser ablation,[12,14] which requires sophisticated instrumentation (such as multi-axis electronically controlled goniometers) and associated processing conditions. Alternative strategies for the fabrication of 3D interconnects that involve 3D printing of metallic inks,[15] fused deposition modelling,[16] hydroprinting of silver nanoparticles,[17] pop-up assemblies created using pre-straining of elastomeric substrates,[18] or networks of liquid metal wires[19] have been reported; however most of these approaches still require specialized instruments (e.g., 3D printers with multiaxial movement) or are limited to certain types of materials. The reported approach circumvents many of these technical necessities.

From a scalability and sustainability standpoint, ECD possesses several distinct advantages in the formation of conformal metallic coatings—characteristics that drove us to use ECD in the current report.[20] The challenge in adapting ECD to patterning traces in 2D and 3D without the aid of lasers-based activation schemes is spatially confining where the chemical processes occur (the use of polydopamine was demonstrated to deposit copper traces on 2D substrates)[21]. Herein, we overcome this challenge through the use of bi-layered microfluidic channel networks, "soft micro-reactors" which were easily sealed via compressive stress, to a range of planar and non-planar surfaces.[1c] We fabricated the "soft micro-reactors" in combinations of a stiff silicone (polydimethylsiloxane, PDMS) and a soft silicone (Ecoflex®) using 3D printing and soft lithography.[22] We could then flow appropriate reagents through the compression-sealed soft micro-reactors to facilitate metallization on the substrate surface, selectively, thus enabling the facile fabrication of conductive traces of desired geometries. Surprisingly, the use of 2D/3D microfluidic systems to pattern metal traces remains unexplored. Compression-based reversible sealing not only allows rapid iterations of chemical depositions (and etching when needed), but also facilitates studying, testing, and use of the conductive traces in functional circuits. Following this strategy, the fabrication of 3D circuits of potential use in numerous electronic devices (e.g., mobile phones, toys, audio devices, etc.) can be made simple and convenient thus making non-planar form factors readily accessible and providing more design flexibility.[20]

Most consumer electronics are made of PCB-based circuitry housed in structural plastics. Here, we focused on the deposition of traces on structural plastics common to these applications: polypropylene (PP), polystyrene (PS), polyethylene terephthalate (PET), fiberglass (FG), polycarbonate (PC), and acrylonitrile butadiene styrene (ABS), as well as those that are not as common—teflon (PTFE) and polyvinylchloride (PVC). In addition to advantages in generating 3D traces, this approach could eliminate the need for dedicated PCBs enabling devices that are more environment friendly by: (i) reducing the amount of material needed to make the devices, and (ii) working exclusively with readily recyclable plastics.[23] We fabricated several different circuits and antennas using these materials to demonstrate the generality of our approach to the fabrication of free-form 3D electronics which collocate mechanical and electrical functionality.

We made use of standard off-the-shelf components in these demonstrations because they are low cost and commercially available with well-established performance characteristics. We chose to produce simple sensors and antennas because they illustrate the utility of the reported method in the practical context of objects produced on mass. Further, when combined with commodity plastics, the function of these circuits could lead to "smart consumables" that are electronically functional, yet cheap enough to be disposable.[23b] Although these are simple circuits, they involve LEDs, capacitors, resistors, transistors, photo-resistors, and batteries, which are essential components found in many electronic devices.

2. Results & Discussion

2.1. Flow-assisted electroless deposition of functional coatings

We deposited conductive copper traces on planar and non-planar substrates of different commodity plastics via electroless deposition using bi-layered microfluidic soft reactors (Fig. 1, Fig. S1, and see S.I. text). We then demonstrated the conductivity of our traces on planar (Fig. 1b) and 3D substrates (Fig. 1c) by attaching surface-mount LEDs (using silver paste) to visually communicate the conductivity of these traces—failure of the LEDs to turn on would indicate discontinuous traces.

To evaluate the application of these traces in the fabrication of electronic circuits, we compared the performance of our traces to traces obtained using established techniques (e.g., those found in PCBs). The resistance of the traces fabricated using microfluidic-directed

ECD (μ-DECD) for different lengths (of constant thickness, 1.5 μm) and different thicknesses (of constant length, 3 cm) was 0.1–8 ohms, which is comparable to the resistance observed in PCBs (0.01–1.5 ohms) (Fig. S2a, b). The differences in the resistance of the traces fabricated following the described approach and those in PCBs could arise from contact resistance between the traces and the measurement probes or the higher density of grain boundaries in ECD traces (Fig. 1d) compared to films deposited using other approaches common to PCBs.[24] For short traces of less than 2 inches, which are preferred in circuit design to reduce electromagnetic interference effects,[25] although the resistance of the traces we report is double compared to the resistance of traces in traditional PCBs, it did not impact the performance. We further determined the microstructure, deposition rate, stability, and adhesion of the traces generated using microfluidic assisted ECD. The granular microstructure of the deposited trace (Fig. 1d) was consistent with the microstructure expected for copper deposition.[26] We measured the deposition rate, using profilometry and confocal microscopy (Fig. 1e), of the process by examining the thickness of traces generated for different deposition times (between 4 and 60 mins) and found a rate of 6.7±1.6 μm/hr (giving traces which ranged in thickness from 1 to 5 μm). These thicknesses are typical of traces deposited via ECD following laser directed structuring (3–10 μm),[14] and of conventional traces in PCBs (10–35 μm).[25]

We observed that the copper traces were stable when the soft reactors were sealed over them, which is critical for subsequent deposition and etching steps (Fig. S3). The copper traces adhered better to textured (e.g., those with a matte finish) polymers when compared to smooth films (Fig. S3b-d), which indicated the importance of surface roughness to the deposition process. We believe that micron-scale surface roughness improved the adhesion of the Pd seeds and thus the copper traces.[13b] We note that despite this result, protective coatings, as required to prevent oxidation in ambient environments, would yield stability in all cases. For example, we coated traces with Deoxit® (a commercially available coat used to increase the stability of metal coatings/traces to oxidation), observing a significant improvement in the stability of the copper traces to surface oxidation (Fig. S4) and also delamination (as indicated by a Scotch tape test, Fig. S3e, f). We believed that the above measurements supported the conclusion that the traces achieved using microfluidic-assisted ECD matched the performance of the traces found in commercial PCBs.

2.2. 2D planar and non-planar substrates: simple circuits

We deposited traces on 2D substrates of different commodity plastics that are commonly used as structural elements for various electronic devices (Fig. 2). We recreated the characteristics (blunt corners, sharp angles, low-radius curves, and other non-rectilinear features such as loops and coils) of copper traces found in PCBs to illustrate the general applicability of μ-DECD. The width of these traces, as defined by the width of the microfluidic channel network, ranged between 170–1850 μm and there was less than a 5% deviation from the dimensions of the initial master used to mold the soft reactors and the produced traces. The traces had radii of curvatures ranging between 1–15 mm and angles between 30–120° and the densest traces we achieved were three traces per mm (170 μm wide traces separated by 360 μm), on par with the dimensions/densities of common PCBs (Fig. 2a, b). Narrower traces could be deposited using reactors fabricated with masters produced via photolithography or other additive manufacturing procedures.[22,27] Although most of the traces we created were continuous (Fig. 2a-h), we could also create discontinuous traces (Fig. 2k-l) using devices that had multiple channel network layers (Fig. 2i-j and Fig. S5). In these examples, we recreated circuit geometries that had previously been used to fabricate a light sensor (Fig. 2i, k) and a simple intercom device (Fig. 2j, l).

The compression-based reversible sealing of the soft bi-layered microfluidic reactors allowed us to perform sequential deposition by reorienting a single device (Fig. 3a, b) or using multiple devices (Fig. 3c). Copper traces with more intricate designs can be generated via sequential functionalization of the substrate (using etchant and/or activator), followed by subsequent rounds of deposition. We used this approach to generate interwoven, discontinuous copper traces that can lead to circuits with smaller footprints noting the following process characteristics: (i) reorienting a single reactor between an activation and an etching phase can generate systematic breaks in the trace without requiring double-layer devices (Fig. 3b), and (ii) aligning multiple different reactors with the substrate for sequential activation, etching, and activation processes enabled the generation of intersecting traces bridged by surface mount components (Fig. 3c, Video S1).

We took advantage of the flexibility of the soft micro-reactors and further applied them to generate conductive traces on embossed substrates (Fig. 4). Matte finish PC films (6 µm, RMS roughness) were embossed to yield corrugated (Fig. 4a, a′), diamond textured (Fig. 4b, b′), or dimpled (Fig. 4c, c′) substrates that encompass a range of surface topographies that would be challenging to pattern with conductive traces using other methods. We determined the vertical offset for the features on these substrates, which varied from a few microns to several hundred microns, using confocal microscopy (Fig. 4a′– c′): corrugated (520 ± 10 µm), diamond textured (940 ± 20 µm), and dimpled (1260 ± 50 µm). Such embossed structures are useful because they impart structural rigidity along multiple or single axes, to otherwise flexible polymer sheets. For example, corrugated surfaces gave an easy bending axis, while the orthogonal axis remained relatively stiff (Fig. 4a). We showed that the circuits were functional when the substrate was flexed along the easy bending axis, illustrating potential applications of our approach to the fabrication of bendable or flexible circuitry.

2.3. 3D substrates: simple LED displays, sensors, and antennas

We used tension to seal our reactors to 3D components and used µ-DECD to produce 3D traces. Specifically, we deposited copper traces on 3D plastic parts with beveled edges (Fig. 5a), positive or/and negative curvature (Fig. 5b, c, e), and variable radii of curvature (Fig. 5d).

The degree of curvature tested using these different components (Fig, 5a-e) ranged from 3–36 mm. The ability to deposit functional, uniform copper traces onto 3D parts using μ-DECD provides clear advantages over methods that rely on laser ablation as the ECD activation step or other direct write methods (in terms of process simplicity and the necessary instrumentation).

We used trace designs that are typical to different types of antennas (e.g., radio-frequency, WiFi), again using LEDs as a direct readout of the continuity of the conductive pathways. Similar to studies on planar materials, multiple activation/etching procedures were possible, and we performed sequential modification (μ-DECD followed by etching) on a hemisphere (Fig. 5e). In addition to circuits involving only LEDs, we also interfaced a range of off-the-shelf electronic components (e.g., capacitors, resistors, transistors, photoresistors, and batteries) to generate functional circuits on 3D plastic parts. We combined through-hole and surface-mount components (including a photoresistor as the detection element) to generate a light sensing circuit on the surface of a polycarbonate hemisphere. When the photoresistor was covered (obstructing incident light), the LED lit up (Fig. 6a, Video S2). This demonstration highlights the strength of μ-DECD in creating 3D circuits that incorporate different off-the-shelf electronic elements—though we focused on this simple demonstration, by extension more elaborate circuits with additional function will be possible and can lead to cheap, reliable production of "smart", disposable, electronic consumables. Furthermore, by enabling the low cost production of 3D traces and circuits on commodity plastic parts, we believe μ-DECD will enable the use of 3D circuit design in an expanding range of contexts.

As another demonstration we used μ-DECD to fabricate compact antennas that mimicked commercially available devices operating in the radiofrequency (MHz) range. We replicated a common radio-frequency identification (RFID) antenna design on a planar (Fig. 6b) and non-planar substrate (Fig. 6c), where the later would be relatively difficult to fabricate using conventional means. The amplitude of the reflection (S_{11}) and transmission (S_{21}) coefficients, also known as S-parameters,[28] of the designed antennas were measured in dB in (Fig. 6e, f) and (Fig. 6g), respectively, by using the E5072A ENA Series Vector Network Analyzer (VNA) from Keysight (Fig. 6d). The reflection coefficients of the antennas (Fig. 6e, f) were found to have values less than -10dB for frequencies below 4 MHz for most antenna geometries, which means that the presented antennas are matched to the surrounding environment and radiate correctly below 4 MHz, which are typical operation frequencies of conventional RFID antennas.[29] In addition, the transmission coefficients measured between two antennas (Fig. 6g) had values larger than -30dB, which consists the threshold value for a successful wireless data transmission,[29] for frequencies above 2 MHz. Hence, these measurements also proved that the presented antennas can efficiently operate in transmission mode. Further the antennas when connected to an Arduino wireless board, enabled the transmission of a near-field communication (NFC) tag that was detected using an application on a smartphone (Fig. S6, Video S3). These experimental demonstrations highlight the direct applicability of µ-DECD to the fabrication of antennas with traditional 2D and non-traditional 3D form factors with applications in communication technologies where the latter can open up new opportunities in the packaging of antennas in consumer electronic devices.

3. Conclusion

We have demonstrated the fabrication of simple circuits and antennas, through direct deposition of conductive traces on various materials of a diverse range of geometries and textures using a process we call µ-DECD. The method we report and its compatibility with off-the-shelf electronic components enables the manufacture of various electronic sensors and circuits in forms, and at cost points not accessible using other techniques. This approach could simplify the production and extend the capabilities of plastic consumables, potentially imbibing new functions to objects with complicated geometries and/or low consumer value that would be difficult or impractical (economically) to impart electronic function to using existing methods (e.g., so called free-form electronics or “smart” consumables).[30] Further, by extending this deposition strategy to other functional inorganic materials, we could construct new variants of plastic/metal hybrid structures not accessible using other strategies. We believe that the strategies and concepts presented herein (as represented by μ-DECD) are applicable to a variety of emerging technologies including: smart textiles,[31] disposable healthcare monitoring systems,[32] self-powered soft robots (including those that use thin polymeric substrates[33] with metallic traces to connect/integrate power sources),[34] antennas,[15a,15c] and passive safety/health sensors.[35]

Supporting Information

Supporting Information is available from the Wiley Online Library or from the author. Supporting information includes experimental details, characterization, and discussion.

Acknowledgements

We thank the Department of Chemistry and the Nebraska Center for Materials and Nano Science (NCMN), at the University of Nebraska–Lincoln, and the University of Nebraska–Lincoln for start-up funds. S.A.M. thanks 3M for support through a Non-Tenured Faculty Award. This work was supported by the National Science Foundation under Grant No. 1555356. Authors thank Bob Rhynalds (Instrument shop, UNL) for help with fabricating templates for textured surfaces, and Dr. Gabriel Hmimina (School of Natural Resources, UNL) for help with Antennas. This research was performed in part at the NanoEngineering Research Core Facility, and at the Nebraska Nanoscale Facility: National Nanotechnology Coordinated Infrastructure and the Nebraska Center for Materials and Nanoscience, which are supported by the National Science Foundation under Award ECCS: 1542182, and the Nebraska Research Initiative.

Received: ((will be filled in by the editorial staff))
Revised: ((will be filled in by the editorial staff))
Published online: ((will be filled in by the editorial staff))

References

[1] a) Q. Chen, G. Li, Y. Nie, S. Yao, J. Zhao, *Microfluid. Nanofluid.* **2014**, *16*, 83; b) J. C. McDonald, M. L. Chabinyc, S. J. Metallo, J. R. Anderson, A. D. Stroock, G. M. Whitesides, *Anal. Chem.* **2002**, *74*, 1537; c) A. Konda, J. M. Taylor, M. A. Stoller, S. A. Morin, *Lab Chip.* **2015**, *15*, 2009.

[2] a) M. Datta, *Electrochim. Acta* **2003**, *48*, 2975; b) F. Lowenheim, in *STP29408S Guide to the Selection and Use of Electroplated and Related Finishes*, DOI: https://doi.org/10.1520/STP29408S, ASTM International, West Conshohocken, PA **1982**, p. 8.

[3] G. A. Krulik, *J. Chem. Educ.* **1978**, *55*, 361.

[4] W. L. Gladfelter, *Chem. Mater.* **1993**, *5*, 1372.

[5] R. Gonzalez, H. Ashrafizadeh, A. Lopera, P. Mertiny, A. McDonald, *J. Therm. Spray Techn.* **2016**, *25*, 897.

[6] C. T. Wan, K. A. Taylor, D. L. Chambers, G. T. Susi, in *Metallized Plastics 2: Fundamental and Applied Aspects* (Ed: K. L. Mittal), Springer US, Boston, MA **1991**, p. 81.

[7] D. Li, K. Goodwin, C.-L. Yang, *J. Mater. Sci.* **2008**, *43*, 7121.

[8] X. Y. Cui, D. A. Hutt, P. P. Conway, *Thin Solid Films* **2012**, *520*, 6095.

[9] a) M. S. Miller, G. J. E. Davidson, B. J. Sahli, C. M. Mailloux, T. B. Carmichael, *Adv. Mater.* **2008**, *20*, 59; b) K.-M. Huang, S.-C. Tsai, Y.-K. Lee, C.-K. Yuan, Y.-C. Chang, H.-L. Chiu, T.-T. Chung, Y.-C. Liao, *RSC Adv.* **2017**, *7*, 51663.

[10] K. Lal Mittal, *Metallized Plastics 2: Fundamental and Applied Aspects*, **1991**.

[11] a) J. Li, P. A. Kohl, *Plating Surf. Finish.* **2004**, *91*, 40; b) M. Paunovic, in *Modern Electroplating*, John Wiley & Sons, Inc. **2010**, p. 433.

[12] a) K. Kordás, J. Békési, R. Vajtai, L. Nánai, S. Leppävuori, A. Uusimäki, K. Bali, T. F. George, G. Galbács, F. Ignácz, P. Moilanen, *Appl. Surf. Sci.* **2001**, *172*, 178; b) X. C. Wang, H. Y. Zheng, G. C. Lim, *Appl. Surf. Sci.* **2002**, *200*, 165.

[13] a) R. L. Meek, *J. Electochem. Soc.* **1975**, *122*, 1177; b) X. Cui, D. A. Hutt, D. J. Scurr, P. P. Conway, *J. Electochem. Soc.* **2011**, *158*, D172.

[14] M. Borges, *Laser Tech. J.* **2014**, *11*, 48.

[15] a) J. J. Adams, E. B. Duoss, T. F. Malkowski, M. J. Motala, B. Y. Ahn, R. G. Nuzzo, J. T. Bernhard, J. A. Lewis, *Adv. Mater.* **2011**, *23*, 1335; b) M. A. Skylar-Scott, S. Gunasekaran, J. A. Lewis, *P. Natl. Acad. Sci. U.S.A.* **2016**, *113*, 6137; c) B. Y. Ahn, E. B. Duoss, M. J. Motala, X. Guo, S.-I. Park, Y. Xiong, J. Yoon, R. G. Nuzzo, J. A. Rogers, J. A. Lewis, *Science* **2009**, *323*, 1590; d) M. A. Cruz, S. Ye, M. J. Kim, C. Reyes, F. Yang, P. F. Flowers, B. J. Wiley, *Part. Part. Syst. Char.* **2018**, DOI: 10.1002/ppsc.2017003851700385.

[16] J. R. Jian, T. Kim, J. S. Park, J. Wang, W. S. Kim, *AIP Adv.* **2017**, *7*, 035314.

[17] G. Saada, M. Layani, A. Chernevousky, S. Magdassi, *Adv. Mater. Technol.* **2017**, *2*, 1600289.

[18] H. Fu, K. Nan, W. Bai, W. Huang, K. Bai, L. Lu, C. Zhou, Y. Liu, F. Liu, J. Wang, M. Han, Z. Yan, H. Luan, Y. Zhang, Y. Zhang, J. Zhao, X. Cheng, M. Li, J. W. Lee, Y. Liu, D. Fang, X. Li, Y. Huang, Y. Zhang, J. A. Rogers, *Nat. Mater.* **2018**, *17*, 268.

[19] a) J.-H. So, J. Thelen, A. Qusba, G. J. Hayes, G. Lazzi, M. D. Dickey, *Adv. Funct. Mater.* **2009**, *19*, 3632; b) J. Park, S. Wang, M. Li, C. Ahn, J. K. Hyun, D. S. Kim, D. K. Kim, J. A. Rogers, Y. Huang, S. Jeon, *Nat. Commun.* **2012**, *3*, 916; c) C. Ladd, J.-H. So, J. Muth, M. D. Dickey, *Adv. Mater.* **2013**, *25*, 5081; d) T. Lijun, J. Karina, W. Tianqi, P. N.

Markus, L. Geng, A. S. Adam, *J. Micromech. Microeng.* **2018**, *28*, 054001; e) T. Lu, E. J. Markvicka, Y. Jin, C. Majidi, *ACS Appl. Mater. Inter.* **2017**, *9*, 22055.

[20] M. T. Sierra, J. Jiménez, E. Andino, J. I. Gárate, J. L. Martín, presented at 2008 International Conference on Advances in Electronics and Micro-electronics, Valencia, Spain, Sept. 29 - Oct. 4, **2008**.

[21] S. Ma, L. Liu, V. Bromberg, T. J. Singler, *ACS Appl. Mater. Inter.* **2014**, *6*, 19494.

[22] Y. Xia, G. M. Whitesides, *Angew. Chem. Int. Edit.* **1998**, *37*, 550.

[23] a) J. L. Yu, E. Williams, M. T. Ju, *IEEE I. Symp. Sust. Sys.* **2009**, 351; b) R. Geyer, J. R. Jambeck, K. L. Law, *Sci. Adv.* **2017**, *3*, e1700782.

[24] a) T. Sun, University of Central Florida,, Orlando, Fla. 2009, xiv; b) N. B. Feilchenfeld, L. H. Walsh, in *Proceedings of the Symposium on High Rate Metal Dissolution Processes* (Eds: M. Datta, B. R. MacDougall, J. M. Fenton), Electrochemical Society **1996**, Ch. 13, p. 202.

[25] H. Zumbahlen, in *Linear Circuit Design Handbook*, Newnes, Burlington **2008**, p. 821.

[26] C. Núñez Aguilar, *Bachelors Report*, Universitat Politècnica de Catalunya, June 2014, **2014**.

[27] M. A. Stoller, A. Konda, M. A. Kottwitz, S. A. Morin, *RSC Adv.* **2015**, *5*, 97934.

[28] D. M. Pozar, *Microwave Engineering*, Wiley, **2004**.

[29] C. A. Balanis, *Antenna theory : analysis and design*, John Wiley, Hoboken, NJ **2005**.

[30] a) G. P. Collins, *Sci. Am.* **2004**, *291*, 74; b) B. L. Risteska Stojkoska, K. V. Trivodaliev, *J. Clean. Prod.* **2017**, *140*, 1454; c) G. Lobaccaro, S. Carlucci, E. Löfström, *Energies* **2016**, *9*, 348; d) L. Dago de, *Phys. World* **1999**, *12*, 31.

[31] a) M. Stoppa, A. Chiolerio, *Sensors* **2014**, *14*, 11957; b) H. Zhao, L. Hou, J. X. Wu, Y. X. Lu, *J. Mater. Chem. C* **2016**, *4*, 7156.

[32] a) A. K. Yetisen, M. S. Akram, C. R. Lowe, *Lab Chip.* **2013**, *13*, 2210; b) D. L. Paul, L. Zheng, L. Zhang, J. P. McGeehan, presented at 2013 IEEE Antennas and Propagation

Society International Symposium (APSURSI), 7-13 July, **2013**; c) S. Amendola, R. Lodato, S. Manzari, C. Occhiuzzi, G. Marrocco, *IEEE Internet Things* **2014**, *1*, 144; d) F. B. Myers, R. H. Henrikson, J. Bone, L. P. Lee, *PLoS One* **2013**, *8*, e70266.

[33] J. M. Taylor, K. Perez-Toralla, R. Aispuro, S. A. Morin, *Adv. Mater.* **2018**, *30*, 1705333.

[34] a) M. Wehner, R. L. Truby, D. J. Fitzgerald, B. Mosadegh, G. M. Whitesides, J. A. Lewis, R. J. Wood, *Nature* **2016**, *536*, 451; b) N. W. Bartlett, M. T. Tolley, J. T. B. Overvelde, J. C. Weaver, B. Mosadegh, K. Bertoldi, G. M. Whitesides, R. J. Wood, *Science* **2015**, *349*, 161; c) S. S. Robinson, K. W. O'Brien, H. Zhao, B. N. Peele, C. M. Larson, B. C. Mac Murray, I. M. Van Meerbeek, S. N. Dunham, R. F. Shepherd, *Extreme Mech. Lett.* **2015**, *5*, 47; d) S. Li, H. Zhao, R. F. Shepherd, *MRS Bull.* **2017**, *42*, 138; e) C. Wang, K. Sim, J. Chen, H. Kim, Z. Rao, Y. Li, W. Chen, J. Song, R. Verduzco, C. Yu, *Adv. Mater.* **2018**, *30*, 1706695.

[35] a) M. S. Mannoor, Z. Jiang, T. James, Y. L. Kong, K. A. Malatesta, W. O. Soboyejo, N. Verma, D. H. Gracias, M. C. McAlpine, *Nano Lett.* **2013**, *13*, 2634; b) D.-H. Kim, N. Lu, R. Ma, Y.-S. Kim, R.-H. Kim, S. Wang, J. Wu, S. M. Won, H. Tao, A. Islam, K. J. Yu, T.-i. Kim, R. Chowdhury, M. Ying, L. Xu, M. Li, H.-J. Chung, H. Keum, M. McCormick, P. Liu, Y.-W. Zhang, F. G. Omenetto, Y. Huang, T. Coleman, J. A. Rogers, *Science* **2011**, *333*, 838; c) M. D. Bartlett, E. J. Markvicka, C. Majidi, *Adv. Funct. Mater.* **2016**, *26*, 8496.

Figure 1. Microfluidic-directed electroless copper deposition (μ-DECD) and trace characterization. (a) Schematic illustration of the μ-DECD process, and (b, c) Photos of the reversible sealing of the micro-reactor to a 2D and 3D part (a plastic sheet and cylinder, where the orange band on the cylinder was used to guide the alignment of the reactor). (d) SEM images showing the granular texture of the traces. (e) Profilometry of the trace profile across a 4 mm long and 1.5 mm wide trace generated using a deposition time of 60 mins.

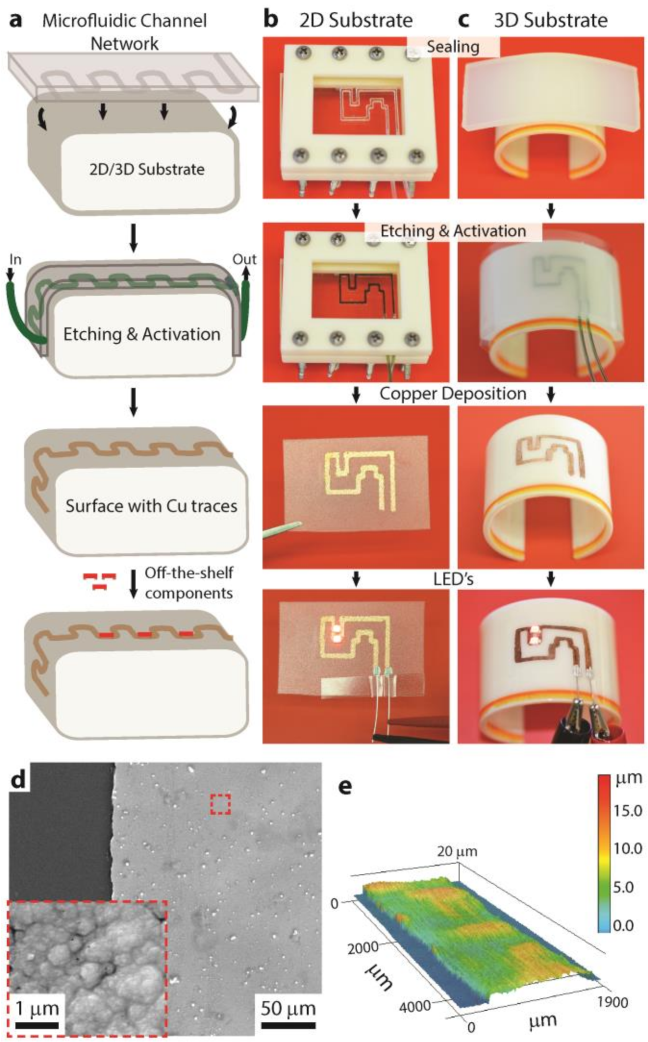

Figure 2. μ-DECD of traces onto different commodity plastic films. Features common to electrical circuit layouts are demonstrated. (a-h) Continuous traces deposited using micro-reactors with single open-ended microchannel networks on: (a-c) polycarbonate (PC, where b is a high-resolution optical image of the traces shown in panel 'a'), (d) polycarbonate with matte finish (PC-M), (e) polypropylene (PP), (f) polystyrene (PS), (g) polyethylene terephthalate (PET), and (h) teflon (PTFE). (i-l) Discontinuous traces deposited using multi-layer micro-reactors (i, j) on: (k) fiberglass (FG) and (l) polyvinylchloride (PVC). The inset images in panels k-l show the contact region of the micro-reactor and the substrate (annotated). Scale bars are 5 mm.

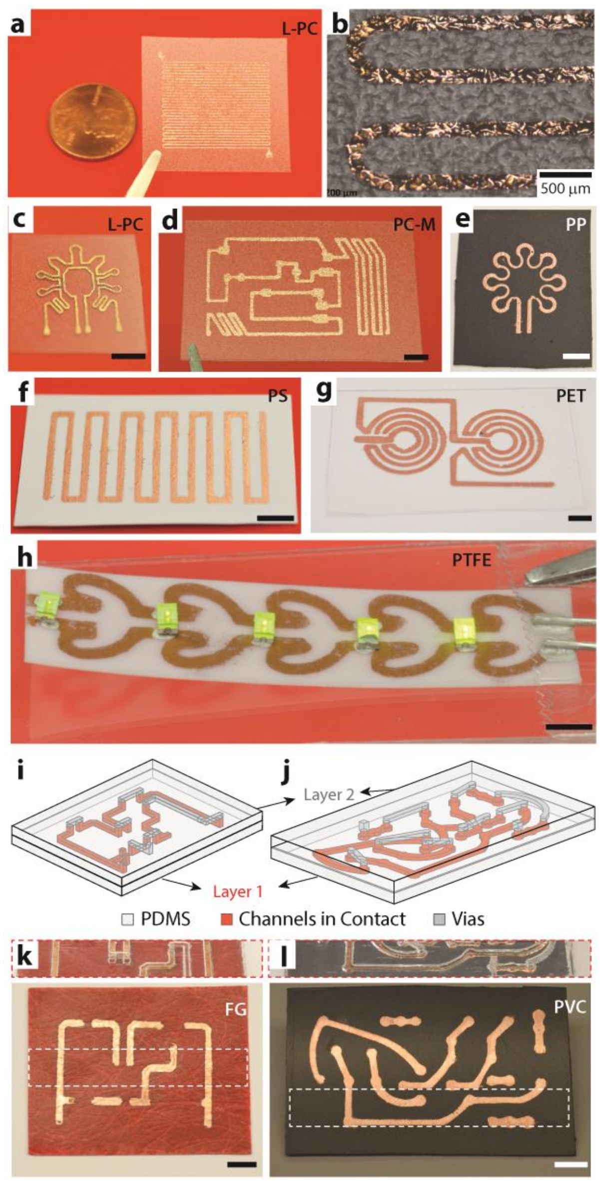

Figure 3. Copper traces fabricated using μ-DECD and sequential deposition/etching. (a) Schematic showing the sequential μ-DECD process: (i) compression sealing and first activation, (ii) second activation/etching, (iii) after copper deposition, and (iv) after attachment and powering of surface-mount LEDs. (b-c) Corresponding photos of the top-down view of the process: (bi, bii, ci, cii, ciii) sealed reactors at different steps of activation (purple) and etching (yellow), (biii, civ) the substrates after copper deposition, and (biv, civ) after attachment and powering the surface mount LEDs. Dyed acetone solutions that etched and colored the surface were used in panels bi, ii, and ci, ii, iii for visualization of the channel design. Scale bars are 5 mm.

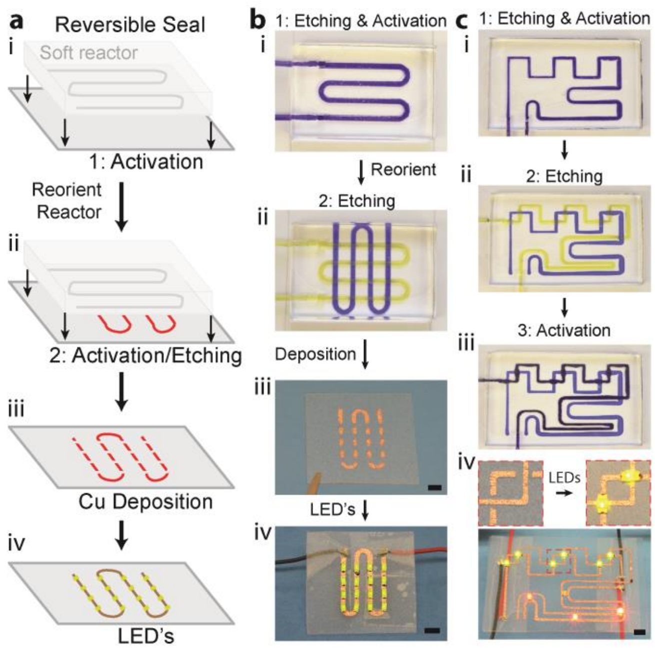

Figure 4. Deposition of conductive traces on embossed substrates using µ-DECD. The surfaces include: (a) corrugated surface, (b) diamond textured surface, and (c) dimpled surface. Surface mount LEDs were attached along the length of the traces. (a′-c′) Surface profiles of the substrates measured using confocal microscopy. Scale bars are 5 mm.

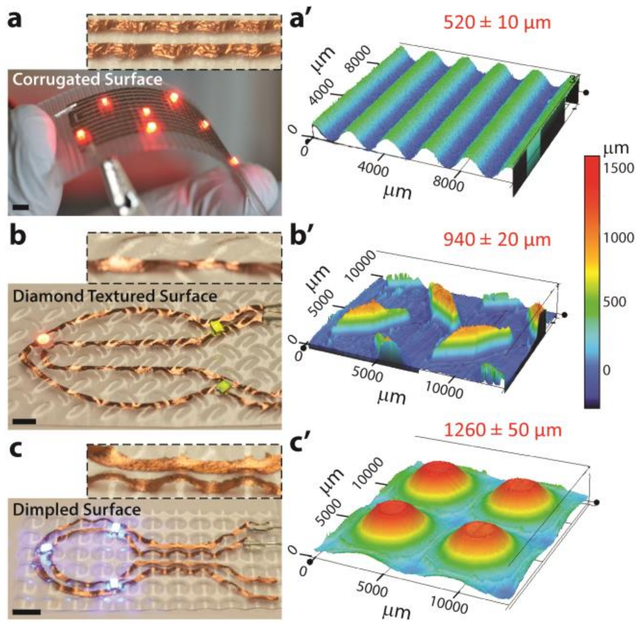

Figure 5. Deposition of conductive copper traces on 3D components using µ-DECD. (a-c) Traces deposited on substrates with 3D geometries (including positive and/or negative curvatures): (a) a square rod with beveled edges, (c) a circular rod, (c) a wedge, (d) a cone, and (e) a hemisphere where the radius of curvature (R) is annotated in each panel. Surface-mount LEDs, powered externally, were used to indicate continuity of the traces. The traces in panel e were fabricated using sequential modification, where the traces were selectively etched (shown in the inset) before the LED's were attached. Scale bars are 5 mm.

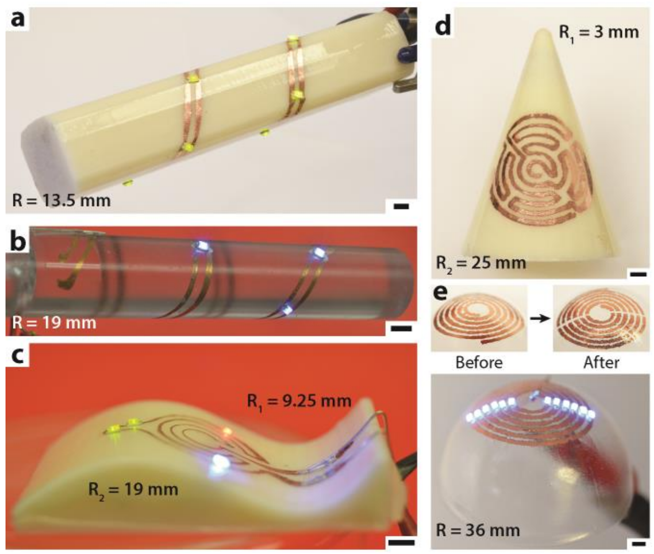

Figure 6. Fabrication of simple sensor circuits and antennas on 2D/3D substrates. (a) Circuit diagram (i) and photos showing a light sensor on a PC after attaching off-the-shelf components (ii, iii). (b, c) Photos of an antenna fabricated using a soft reactor on a planar substrate (b) and a non-planar substrate (c). (d) Set-up showing an antenna connected to a vector network analyzer. (e, f) Radio frequency response (reflectance S_{11} mode) for an antenna ‘‘printed“ on a planar substrate (e), and a comparison with a similar trace on a non-planar substrate (f). (g) Radio frequency response (transmission S_{21} mode) between traces on planar substrates. Scale bar: 5 mm.